



Synthesis, biological assays and QSAR studies of *N*-(9-benzyl-2-phenyl-8-azapurin-6-yl)-amides as ligands for A₁ adenosine receptors

Irene Giorgi^{a,*}, Michele Leonardi^b, Daniele Pietra^c, Giuliana Biagi^a, Alice Borghini^b, Ilaria Massarelli^d, Osele Ciampi^e, Anna Maria Bianucci^a

^a Dipartimento di Scienze Farmaceutiche, Università di Pisa, via Bonanno, 6, 56126 Pisa, Italy

^b Dipartimento di Chimica Bioorganica e Biofarmacia, Università di Pisa, via Bonanno, 33, 56126 Pisa, Italy

^c Centro Interdipartimentale di Ricerche in Farmacologia Clinica e Terapia Sperimentale, via Roma, 55, 56126 Pisa, Italy

^d Dipartimento di Chimica e Chimica Industriale, Università di Pisa, Via Risorgimento 35, 56126 Pisa, Italy

^e Dipartimento di Psichiatria, Neurobiologia, Farmacologia e Biotecnologie, Università di Pisa, via Bonanno, 6, 56126 Pisa, Italy

ARTICLE INFO

Article history:

Received 2 October 2008

Revised 19 January 2009

Accepted 25 January 2009

Available online 31 January 2009

Keywords:

Adenosine receptor ligands

2-Phenyl-9-benzyl-8-azapurines

QSAR, regression

Classification

ABSTRACT

2-Phenyl-9-benzyl-8-azapurines, bearing at the 6 position an amido group interposed between the 8-azapurine moiety and an alkyl or a substituted phenyl group, have been synthesised and assayed as ligands for adenosine receptors. All the compounds show high affinity for the A₁ adenosine receptor, and many of them also show a good selectivity for A₁ with respect to A_{2A} and A₃ adenosine receptors. Based on the quite rich library containing such compounds and relevant biological data, QSAR models, able to rationalise the results and to give a quantitative estimate of the observed trends were also developed. The obtained models can assist in the design of new compounds selectively active on A₁ adenosine receptor.

© 2009 Elsevier Ltd. All rights reserved.

1. Introduction

Adenosine is an important endogenous regulator present in extracellular space in high concentration during metabolically stressful conditions, such as in injury, ischemia and inflammation. It is a powerful signalling molecule that participates in the regulation of a wide variety of physiological and pathophysiological processes mainly addressed to tissue protection and repair.¹ Four adenosine receptors subtypes were identified and cloned: A₁, A_{2A}, A_{2B} and A₃. Up to now many ligands targeting the adenosine receptor subtypes have been synthesised and developed but none of them has reached clinical applications. Nevertheless, the interest on designing ligands with high activity and selectivity for these receptors is always strong due to the interesting therapeutic perspectives foreseen.²

In the past we obtained a number of ligands of A₁ and A₃ adenosine receptors by modifying the substituent at the 2, 6 and 9 positions of purine and 8-azapurine nucleus. A phenyl ring at the 2 position and a benzyl group at 9 position were found to be good substituents to ensure binding with A₁ and A₃ receptors but not for A_{2A} ones. For A₁ receptors, we showed that cycloalkylamino, alkylamino and alkyl-phenylamino groups, bearing or not a hydroxyl function, are the best substituents for C(6) (Fig. 1 A).^{3–6} A phe-

nyl-ureido function at the same position was found to shift the affinity towards A₃ receptors (Fig. 1 B).⁷ So, we have judged that preparing and assaying 2-phenyl-9-benzyl-8-azapurines, bearing, at the 6 position, an amido group interposed between the 8-azapurine moiety and an alkyl, a cycloalkyl, a phenyl or substituted phenyl group or an heterocyclic ring (Fig. 1 C), could be of big interest in view of assaying the effect of the amido function on the affinity of such molecules toward A₁, A_{2A} and A₃ receptors.

We have also believed that the library of compounds acting at the above receptor subtypes, available in our laboratory, had become large enough to allow the development of good QSAR models, to be subsequently exploited with predictive purposes. A very wide variety of approaches are available nowadays for QSAR treatment of biological data. The choice of the most suitable ones strictly depends upon the type of data to be analysed. In this study two different biological indicators of the receptor affinity had to be handled: (1) percentage inhibition of specific binding of radioligand (%i), as in the case of data referring to the A_{2A} and A₃ receptor subtypes, and (2) inhibition constant (K_i), as in the case of data referring to the A₁ subtype. A *multiple linear regression* (MLR) method was used for developing the model enabling activity predictions with regard to the A₁ subtype, while a *data mining* approach, based on *decision trees*, was used for developing the QSAR model enabling activity predictions concerning the A_{2A} and A₃ subtypes. In both cases high quality predictive models were obtained.

* Corresponding author. Tel.: +39 0502219549; fax: +39 0502219605.
E-mail address: igiorgi@farm.unipi.it (I. Giorgi).

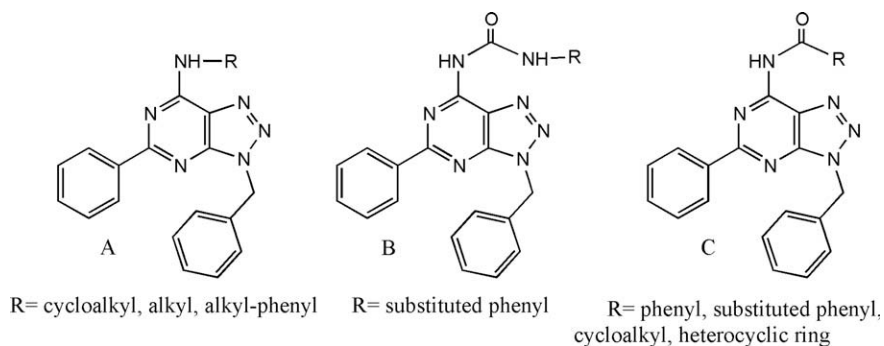
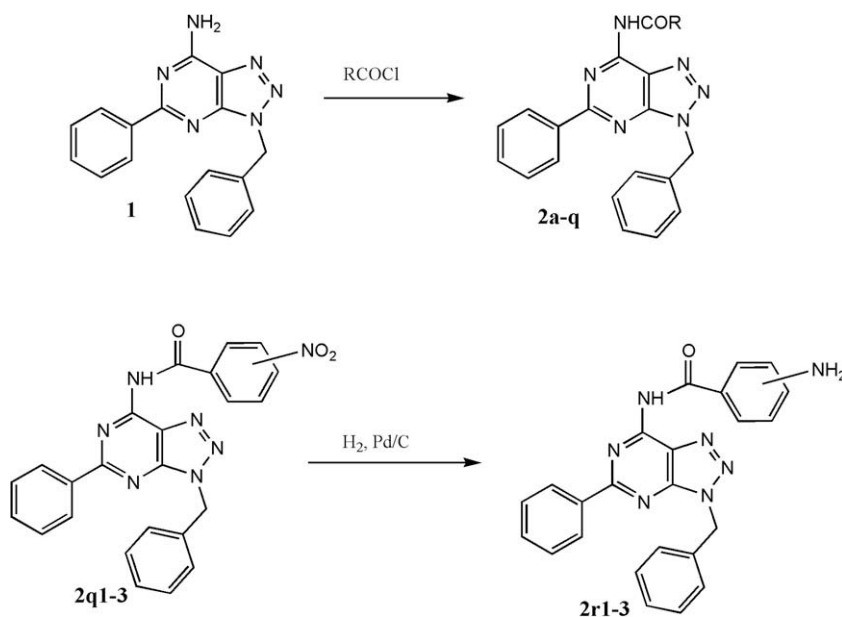


Figure 1. Chemical structures of 2-phenyl-9-benzyl-8-azaadenines (A), 2-phenyl-9-benzyl-N⁶-(arylcabamoyl)-8-azaadenines (B), N-(9-benzyl-2-phenyl-8-azapurin-6-yl)-amides (C).



Scheme 1. General method for the synthesis of compounds **2a-r**.

2. Chemistry

In the Scheme is depicted the general method to obtain compounds **2a-q** and **2r** (Scheme 1).

2-Phenyl-9-benzyl-8-azaahypoxanthine,⁸ obtained by the procedures described,⁹ was transformed by reaction with phosphorus oxychloride (POCl₃) in the corresponding chloride which was not characterised and reacted with NH₃ to give the corresponding adenine **1**.⁶ Compound **1** reacted with the suitable acyl chlorides, prepared from the corresponding acids and thionyl chloride, to give the desired products **2a-q**. In many cases the yield of the reaction was not high probably due to a very low basic character of the N⁶ of 8-azapurines, being the lone pair delocalised in aromatic rings. However the yields were not a problem because the starting compounds are not expensive and we could obtain enough amount of final products to perform chemical analysis and biological assays. Compounds **2q1-3** were reduced with hydrogen and 10% Pd/C at room pressure and temperature to give the compounds **2r1-3**.

3. Biological assays

All new compounds obtained were tested in radioligand binding assays for affinity toward A₁, A_{2A}, and A₃ adenosine receptors. The results are reported in Table 1; when the percentage of inhibi-

tion resulted <60% at 10 μM, compounds were considered inactive. Compound **2h3** has not been assayed because of its low solubility both in DMSO and in the assay buffer Tris-HCl 50 mM, pH 7.4.

For tests involving the A₁ receptors the radiolabelled antagonist [³H]DPCPX was used, while the antagonist radioligand [³H]ZM241385 was used in the experiments involving A_{2A} receptors. In the case of A₃ receptors the agonist radioligand [³H]NECA was used as a probe. The results are given as K_i ± SEM (nM) and/or percentage inhibition of the radioligand, where control binding is 0% and non-specific binding is 100%.

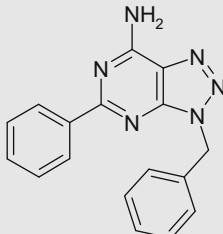
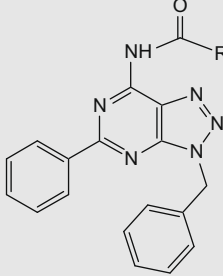

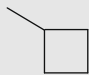
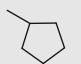
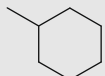
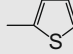
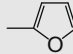
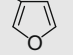
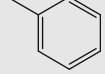
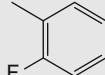
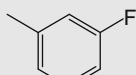
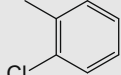
4. Development of QSAR models

The development of QSAR models was carried out in accordance with the guidelines *Guidance document on the validation of (Quantitative) Structure-Activity Relationship [(Q)SAR] models*, OECD Environmental Health and Safety Publications, Series on Testing and Assessment No. 69, 2007.

4.1. Endpoint selection

In this work, compounds have been tested for their A₁, A_{2A} and A₃ adenosine receptor affinity. More in detail, two different indicators of the receptor affinity were collected: (1) percentage inhibi-

Table 1
Molecular structures and biological assay results of compounds towards adenosine A₁, A_{2A} and A₃ receptors

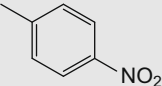
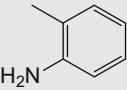
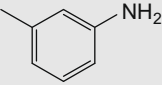
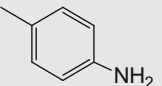
CompdID	Structure	Percentage inhibition of specific binding of radioligand %i ^a and K _i ± SEM (nM) of selected compounds		
		Adenosine A ₁ receptor	Adenosine A _{2A} receptor	Adenosine A ₃ receptor
1		5.6 ± 1.0	147 ± 64	4219 ± 3310
				
	R			
2a		7.5 ± 1.3	110 ± 20	48%i
2b		2.2 ± 0.6	119 ± 29	3033 ± 2518
2c		2.5 ± 0.4	27%i	4686 ± 1121
2d		12 ± 2	40%i	24%i
2e		8.0 ± 0.6	305 ± 90	2290 ± 1735
2f1		12 ± 3	573 ± 25	3047 ± 2053
2f2		10 ± 2	161 ± 38	1637 ± 448
2g		110 ± 13	36%i	15%i
2h1		40 ± 10	35%i	5303 ± 1461
2h2		22 ± 6	21%i	5812 ± 1453
2i1		141 ± 36	38%i	410 ± 170

(continued on next page)

Table 1 (continued)

CompdID	Structure	Percentage inhibition of specific binding of radioligand % ⁱ and K _i ± SEM (nM) of selected compounds		
		Adenosine A ₁ receptor	Adenosine A _{2A} receptor	Adenosine A ₃ receptor
2i2		70 ± 11	0%i	5338 ± ± 400
2i3		108 ± 13	30%i	3547 ± 211
2j		482 ± 119	41%i	103 ± 20
2k1		1523 ± 500	13%i	51%i
2k2		93 ± 20	12%i	5531 ± 975
2k3		28 ± 4	17%i	5288 ± 775
2l		709 ± 84	21%i	56%i
2m1		550 ± 74	27%i	560 ± 45
2m2		163 ± 16	31%i	2506 ± 317
2m3		123 ± 34	39%i	4209 ± 156
2n		1845 ± 765	48%i	51%i
2o		7153 ± 722	31%i	22%i
2p		2143 ± 491	18%i	40%i
2q1		207 ± 14	30%i	41%i
2q2		77 ± 14	6%i	4852 ± 2000

Table 1 (continued)

CompdID	Structure	Percentage inhibition of specific binding of radioligand %i ^a and K _i ± SEM (nM) of selected compounds		
		Adenosine A ₁ receptor	Adenosine A _{2A} receptor	Adenosine A ₃ receptor
2q3		24 ± 7	26%i	57%i
2r1		34 ± 10	297 ± 36	4107 ± 1447
2r2		32 ± 9	4%i	59%i
2r3		7.1 ± 0.7	50%i	926 ± 269

^a Data are expressed as means from 2 to 3 independent experiments performed in duplicate; individual values varied less than 15%.

tion of specific binding of radioligand (%i) and (2) inhibition constant (K_i), as described in 'Biological assays' section in 'Materials and Methods' and in 'Results and discussion'. Compounds and activity values are summarised in Table 1. Different endpoints were rationally selected on the basis of different biological behaviour of the assayed molecules.

All of the assayed compounds turned out to be good ligands for the A₁ adenosine receptor subtypes, which enabled measuring K_i values. Consequently, the affinity of such compounds, expressed in terms of K_i values, supplied the proper endpoint values in the case of data referring to the A₁ subtype. In contrast, most of the analysed compounds were found to be, in the average, poorer ligands for the A_{2A} and A₃ receptors subtypes, so that only %i values were collected for all of them, while K_i values were measured only for most active compounds (i.e., the ones showing %i >60% at 10 μM). Consequently, affinities of compounds toward the A_{2A} and A₃ subtypes, expressed as %i values, supplied the proper endpoint values for such receptor subtypes. It may be worth to point out here that expressing affinity data toward the A_{2A} and A₃ subtypes in terms of %i (measured at 10 μM) offered the advantage that both active and inactive compounds were considered in model building, so ensuring a very wide sampling of the biological indicator.

4.2. Dataset building

A Dataset (DS) containing the 31 compounds reported in Table 1 was considered as the starting point. Subsequently, selected endpoints were subjected to simple mathematical transformations in order to let them assume a proper distribution. The A₁ endpoint (K_i) was converted into pK_i ($-\log K_i$) in order to have normally distributed property values. The reader is referred to http://en.wikipedia.org/wiki/Normal_distribution and related links for a definition of normal distribution.

As explained in more detail later, the development of a model by means of a multiple linear regression requires that the above assumption is fulfilled. The A_{2A} and A₃ endpoint (%i) was discretized into two classes ('Inactive' and 'Active') as follows:

- the 'Inactive' class contains compounds with %i at 10 μM < 60%
- the 'Active' one contains compounds with %i at 10 μM ≥ 60%

Table 2 illustrates all the 31 compounds together with pK_i values for A₁ receptor as well as the 'Inactive' or 'Active' class for A_{2A} and A₃ receptors.

4.3. Molecular descriptor calculation

For each compound belonging to DS, 149 molecular descriptors were calculated starting from molecular structures expressed in terms of 'molecular graphs' (drawn in MDL IsisDraw 2.5). Such descriptors account for molecular features of bi-dimensional (2D) type. These descriptors may be easily calculated by most of the computer programs suitable for molecular descriptor calculation. In this work, they were specifically calculated by using software developed 'in house'. Such descriptors consist of constitutional descriptors, information indices, topological indices and charge descriptors. Among all molecular descriptors calculated, a selection of the ones which showed a normal distribution was made first, as required for proper development of a multiple linear regression model, and for the purpose of defining the applicability domain of the model in terms of range of molecular descriptor values. The normal distribution of descriptors was tested by the Kolmogorov-Smirnov test.¹⁰

4.4. Splitting of dataset into training set and test set pairs

It may be worth to recall here a crucial point in QSAR model development. Any QSAR model is developed ('trained') over a dataset containing known molecular structures and relevant biological property values ('training' set or TR set). The model needs then to be validated on a smaller dataset (not less than 1/5 of TR set) also containing known molecular structures and relevant biological property values ('test' set or TS set). TR and TS are sub-sets belonging to the initial DS previously mentioned. They must be obviously (fully) disjointed with respect to each other, in order to enable the so-called 'external validation' of the QSAR model itself. Indeed, if molecular structures and relevant biological property values (target property) are properly sampled, statistical parameters, arising from comparison between computed and experimental target property values enable quantifying the predictive power of the model. It has also to be taken into account that any QSAR model gives valid predictions only if the molecules, to be predicted by it, fall into the chemical space defined by the specific 'training set' (TR set), where such a model has been developed, i.e. fall into the so-called Applicability Domain (AD) of the QSAR model itself. Based on what mentioned above, rational splitting of the initial DS into suitable TR/TS set pairs, so that every point (compound) of the TS is closed to at least one point (compound) of the TR, in the chemical space

Table 2
Summary of actual and predicted affinity values towards adenosine A₁ receptor and actual and predicted affinity class towards A_{2A} and A₃ receptors, for all the analysed compounds, together with their belonging to TR or TS, and with molecular descriptors involved in the models

Compd ID	TR/TS	A ₁ actual pK _i	A ₁ predicted pK _i	A _{2A} actual class	A _{2A} predicted class	A ₃ actual class	A ₃ predicted class	RπID-TPC	B6HES	J ₈	MIC ₀
1	TR	8.25	8.43	Active	Active	Active	Active	62.933	2.879	0.007	1.472
2a	TR	8.12	8.38	Active	Active	Inactive	Active	63.987	3.067	0.007	1.549
2b	TS	8.65	8.44	Active	Active	Active	Active	67.39	3.107	0.006	1.532
2c	TR	8.61	8.27	Inactive	Inactive	Active	Active	70.734	3.149	0.006	1.515
2d	TS	7.91	7.87	Inactive	Inactive	Inactive	Inactive	74.013	3.193	0.007	1.498
2e	TR	8.1	7.88	Active	Active	Active	Active	78.361	3.12	0.006	1.662
2f1	TR	7.93	7.88	Active	Active	Active	Active	78.361	3.121	0.006	1.619
2f2	TS	8	7.88	Active	Active	Active	Active	78.361	3.116	0.006	1.619
2g	TR	6.96	7.28	Inactive	Inactive	Inactive	Inactive	85.568	3.16	0.007	1.521
2h1	TR	7.4	6.51	Inactive	Inactive	Active	Active	91.665	3.16	0.009	1.634
2h2	TR	7.66	7.32	Inactive	Inactive	Active	Active	84.757	3.164	0.007	1.634
2i1	TR	6.85	6.51	Inactive	Inactive	Active	Active	91.665	3.16	0.009	1.634
2i2	TR	7.16	7.32	Inactive	Inactive	Active	Active	84.757	3.162	0.007	1.634
2i3	TS	6.97	7.09	Inactive	Inactive	Active	Active	84.784	3.164	0.008	1.634
2j	TR	6.32	6.51	Inactive	Inactive	Active	Active	91.665	3.16	0.009	1.634
2k1	TS	5.82	6.22	Inactive	Inactive	Inactive	Inactive	97.355	3.16	0.009	1.576
2k2	TR	7.03	7.05	Inactive	Inactive	Active	Active	90.044	3.199	0.007	1.576
2k3	TR	7.55	7.16	Inactive	Inactive	Active	Active	83.494	3.212	0.008	1.576
2l	TR	6.15	7.09	Inactive	Inactive	Inactive	Inactive	84.784	3.203	0.008	1.507
2m1	TR	6.26	6.06	Inactive	Inactive	Active	Active	95.964	3.182	0.01	1.742
2m2	TR	6.79	6.89	Inactive	Inactive	Active	Active	88.626	3.226	0.008	1.742
2m3	TS	6.91	7.01	Inactive	Inactive	Active	Active	81.789	3.236	0.009	1.742
2n	TR	5.73	6.17	Inactive	Inactive	Inactive	Inactive	102.75	3.329	0.008	1.56
2o	TR	5.15	6.24	Inactive	Inactive	Inactive	Inactive	96.89	3.164	0.009	1.684
2p	TS	5.67	5.88	Inactive	Inactive	Inactive	Inactive	99.471	3.34	0.01	1.781
2q1	TR	6.68	6.08	Inactive	Inactive	Inactive	Inactive	99.964	3.334	0.009	1.674
2q2	TR	7.11	6.95	Inactive	Inactive	Active	Active	92.055	3.296	0.007	1.674
2q3	TS	7.62	7.09	Inactive	Inactive	Inactive	Active	84.68	3.286	0.008	1.674
2r1	TS	7.46	6.51	Active	Inactive	Active	Inactive	91.665	3.16	0.009	1.547
2r2	TR	7.5	7.32	Inactive	Inactive	Inactive	Inactive	84.757	3.175	0.007	1.547
2r3	TS	8.15	7.09	Inactive	Inactive	Active	Inactive	84.784	3.187	0.008	1.547

defined by molecular descriptors, is one of the most critical steps in developing QSAR models.

In this work, selection of the TR/TS couple was carried out as follows: DS molecules were first classified by using a hierarchical clustering algorithm.¹¹ In hierarchical clustering, data are iteratively partitioned, until convergence is reached. Proceeding molecule by molecule, each step of the clustering is characterised by the creation of a tree which contains molecules at its leaves and the whole DS at the root node. The method used herein is a commonly known agglomerative method, where molecules are added one by one and the forming tree is opportunely updated at each step, assigning each examined compound to most appropriate leave, i.e. cluster. At each stage the method merges the two clusters which are closest (i.e. most similar) to each other. The 'choice' of the cluster to be assigned to a particular molecule was made in this work by using the 'average linkage clustering' method, where the distance (or similarity) between clusters is defined as the average distance, i.e. the average of the distances, between each object (compound) of the first cluster and each object (compound) of the second cluster.

In this way, five clusters were obtained, two of which have only one compound, the other clusters have 8, 8 and 13 compounds, respectively. Secondly, individual TS molecules were extracted from each cluster with more than one compound, by randomly selecting about 30% of the molecules belonging to each cluster. All the selected molecules constituted the test set, while all the remaining molecules made up the training set. As a result, the present DS with 31 entities in all, was split into a TR with 21 compounds and a TS with 10 compounds, as summarised in Table 2.

All of the obtained QSAR models were also compared with corresponding models wherein the TR/TS couples were randomly selected. In this case too, 21 compounds were assigned to TR and 10 compounds to TS.

4.5. Model building

A method based on *multiple linear regression (MLR)* was used for developing the model enabling activity predictions with regard to A₁ receptor subtypes. The general purpose of multiple linear regression is to relate the dependent variable *y* (biological activity) to a number of independent variables *x_i* (molecular descriptors) by using a linear equation such as

$$y = a + b_1 * x_1 + \dots + b_i * x_i$$

where *a* is the intercept and *b_i* is the *i*th regression coefficient. In order to safely apply the MLR method of correlation, some assumptions need to be fulfilled, such as

- data have to be continuous
- variables must have a normal distribution
- independent and dependent variables must be linearly related
- assumption of homoscedasticity
- residual errors have to be normally distributed.

The data treated in building the QSAR models described here fulfilled the above assumptions.

A *data mining* approach which makes use of the *C4.5 decision trees* was used for developing the QSAR model enabling activity predictions with regard to the A_{2A} and A₃ receptor subtypes. This approach does not require that assumptions regarding data distribution are satisfied. Decision trees were built to evaluate possible relationships between molecular features (expressed in terms of molecular descriptors) and biological activity within the two classes, 'Active' and 'Inactive', for both receptor subtypes. The construction of a decision tree is a recursive operation which first selects a descriptor (numeric) to be placed at the root node by comparing it with a predetermined constant value, so making a

binary split (also called two-way split) depending on whether the descriptor value is higher or lower/equal than that constant. Descriptors to be used for splitting are determined by the information gain, a statistical property measuring the homogeneity of each daughter node. Descriptors providing a higher value of information gain will afford more homogeneous nodes and will be selected to build the tree. In contrast, descriptors providing low values of information gain will be discarded, that way leading to a pre-selection of descriptors to be included in tree construction. This operation allows splitting the TR into two branches, so leading to two subsets, according to threshold defined by the constant. Such a step can be then recursively repeated for each branch, finally resulting in leaf nodes which represent classification. A molecule is classified following down the tree along its branches, according to the values of descriptors in the successive nodes. When that molecule reaches a leaf, the class assigned to that leaf will also be assigned to the molecule.¹² The iterative repetition of assignments for all the TR molecules gave the decision tree models for affinity on A_{2A} and A₃ adenosine receptors.

4.6. Statistical validation of the models: assessment of goodness of fit, robustness and predictive ability

Goodness of fit, robustness and predictive ability of the developed models were used herein as statistical measures of performance of the models themselves.

The term 'goodness of fit' is intended to mean how well the model predicts compounds belonging to TR. The term 'robustness' indicates the stability of the model, and consequently the one of predictions obtained by it, when changes are introduced in the TR and the model is re-trained taking into account these changes. It may be assessed by leave-one-out cross-validation (LOO-CV), in which each compound is in turn left out of the TR, so that each new reduced TR is used to develop a model enabling classification of each compound left out. The term 'predictive ability' means how well the model predicts compounds belonging to the external TS. The obtained models were also submitted to response permutation tests (as described in the above mentioned OECD guidelines, page 52–53 and references cited therein) in order to verify the absence of chance correlation.

For the regression model developed at A₁ receptor, all the above-mentioned assumptions were observed. Moreover, among parameters commonly used in model validation, the statistical parameters which give a measure of performance of the model are reported in Table 3. On regard to the models concerning activity at the A_{2A} and A₃ receptors, the results of the classification may be organised in a confusion matrix. Confusion matrix (also called contingency matrix) shows actual classes in rows and classes, predicted by the classifier, in columns. The main diagonal represents the numbers of correctly classified molecules, that is, cases where in the actual class is the same as the predicted class; in contrast, numbers out of the main diagonal represent misclassifications.

Table 3

Model validation on adenosine A₁ receptor. Statistical parameters coming from training set, leave-one-out cross validation and test set, respectively

TR	LOO	TS
Residual sum of squares SSRES	4.37	Predictive residual sum of squares PRESS 5.68
Multiple correlation coefficient R ²	0.72	Predictive residual sum of squares PRESS 2.60
Multiple correlation coefficient R ² by permutation test	0.088	Multiple correlation coefficient R ² 0.70
Number of predictor variables	2	Multiple correlation coefficient R ² —
Number of observation	21	Number of predictor variables 2
Adjusted R ²	0.68	Number of observation 21
Standard error of estimate	0.49	Number of observation 10
F-Value	22.70	Adjusted R ² 0.61
Standard deviation error of estimate	0.46	Standard error of prediction 0.61
		F-Value 8.15
		Standard deviation error of prediction 0.51
		SDEP

The most significant statistical parameters are reported, which may be obtained from values included within confusion matrices. In particular, sensitivity, specificity, concordance, positive predictivity, negative predictivity, false positive rate, and false negative rate constitute the Cooper statistics,¹³ while the remaining parameters are the ones commonly used in model validation. Such parameters refer to TR, LOO-CV and TS classifications.

4.7. Estimate of applicability domain of the models

In the cases of all the three models, TS molecules were selected so that they belonged to the applicability domain of the model, which is determined by TR molecules. Several different methods enabling to define the applicability domain are available. They have been recently reviewed in Jaworska et al.¹⁴

In this work, a double check was performed. First of all, all TS molecules were verified to possess a 2-phenyl-9-benzyl-8-azaadenine substructure. This is because the models were developed with the aim of screening new libraries of compounds bearing such moieties, which obviously drove the selection of the TR molecules. Then the range of values taken by each individual descriptor for TR molecules was considered to define the applicability domain for each model, since descriptors involved in them had shown to be 'normally' distributed.

5. Results and discussion

5.1. Biological results

Biological results demonstrated that the synthesised compounds possess a very interesting affinity toward A₁ receptors, either the ones having an alkyl or cycloalkyl group bound to the carbonyl carbon, or the ones having a phenyl or a substituted phenyl at the same position. On the contrary, the new compounds are in general not significantly active on A_{2A} and A₃ receptor subtypes. Thus, such new compounds possess good selectivity properties toward A₁ receptor with respect to A_{2A} and A₃ receptors.

5.2. QSAR study of A₁ adenosine receptor ligands

The following equation defines the QSAR model developed on A₁ adenosine receptor:

$$pK_i = 13.2595 - 0.0509(\pm 0.0104) * R\pi ID-TPC - 231.3828(\pm 95.376) * J_8$$

where each descriptor is reported with its regression coefficient (\pm standard deviation of the estimated regression coefficient). The model is based on multiple linear regression. It was developed on a total of 21 instances, that is, 21 compounds belonging to TR. Descriptors involved in this model are R π ID-TPC and J₈. R π ID-TPC is the difference between Randic conventional bond-or-

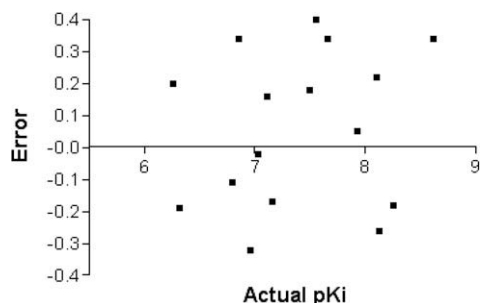


Figure 2. Plot illustrating the trend of errors versus actual pK_i values.

der (π) ID number and total path count.^{15,16} J_8 is the Gavez mean topological charge index of 8 order.¹⁷ Since $R\pi$ ID-TPC values are positive real numbers, lower values of $R\pi$ ID-TPC correspond to higher affinity values. This descriptor reflects features linked to steric hindrance in the molecule. $R\pi$ ID-TPC values increase according to the following scale: no substituent < cyclopropyl < cyclobutyl < cyclopentyl < cyclohexyl < aromatic five-membered rings < aromatic six-membered rings. Concerning the substitution pattern of phenyl ring, the *para* and *meta* positions appear to be preferred, while the *ortho* position is not, due to steric hindrance reasons. Particularly unfavoured are large substituents at the *ortho* position. Since J_8 values are positive real numbers, lower values of J_8 correspond to higher affinity values. This descriptor accounts for both steric and electronic features of compounds. According to such trend, a substituent with optimal size is a 4- or 5-membered ring. Concerning the substitution pattern of phenyl ring, electron-withdrawing groups at *meta* positions are preferred. Mono-substitution at *ortho* positions and di-substitution are not allowed.

Normal distribution of variables and errors (according to the Kolmogorov–Smirnov test), as well as homoscedasticity criteria were observed (see plot in Fig. 2).

The model was developed on compounds belonging to a TR with regard to which a well representative TS set was selected. It was then validated by means of leave-one-out cross-validation (LOO-CV) and by using the external test set (TS). Statistical parameters resulting from LOO-CV and TS validations are reported in Table 3. The applicability domain of this model, calculated on the basis of descriptor ranges, is summarised as follows:

$R\pi$ ID-TPC values: from 62.933 to 102.75 and J_8 values: from 0.006 to 0.01.

5.3. QSAR study of A_{2A} adenosine receptor ligands

The QSAR model developed on A_{2A} adenosine receptor is a J48 pruned tree, with an overall size of 3 and 2 leaves. It can be easily represented in the form of the rules reported below:

Rule 1:

B6HES \leq 3.121
 \rightarrow class Active (4/0)

Rule 2:

B6HES $>$ 3.121
 \rightarrow class Inactive (17/0)

The numbers in parentheses represent the number of compounds predicted to belong to the corresponding class (on the left) and the number of misclassified molecules (on the right, zero in both cases). The only descriptor involved in this model is B6HES, that is, burden sixth highest eigenvalue weighted by Sanderson electronegativities.^{18,19} It reflects both steric and electronic features of compounds, where steric hindrance mostly affects affinity. In particular, a preference scale for substituents is the one which follows: no substituents = cyclopropyl > cyclobutyl > aromatic five-membered rings > cyclopentyl = cyclohexyl = phenyl, the latter one fitting worst in the receptor. Concerning the substitution pattern of phenyl ring, it may modulate affinity, but it does not seem to lead to high affinity compounds.

Also in this case, the applicability domain of the model was calculated on the basis of the range of descriptor values, i.e. B6HES values must range from 2.879 to 3.34.

Confusion matrices concerning the QSAR model for A_{2A} adenosine receptor are illustrated in Table 4, left column. The most significant statistical parameters for the A_{2A} model are reported in Table 5, left column.

5.4. QSAR study of A_3 adenosine receptor ligands

The QSAR model developed on A_3 adenosine receptor also relies on a J48 pruned tree, with an overall size of 7 and 4 leaves. It can be

Table 4

Confusion matrices concerning QSAR models for adenosine A_{2A} (left) and A_3 (right) receptors, calculated on the basis of TR, LOO and TS, respectively

A_{2A} training set	2×2 contingency table			A_3 training set	2×2 contingency table				
			Predicted class				Predicted class		
			Active		Inactive			Active	Inactive
Actual class	Active	4	0	Actual class	Active	14	0		
	Inactive	0	17		Inactive	1	6		
A_{2A} LOO	2×2 contingency table			A_3 LOO	2×2 contingency table				
			Predicted class				Predicted class		
			Active		Inactive			Active	Inactive
Actual class	Active	3	0	Actual class	Active	11	3		
	Inactive	1	17		Inactive	4	3		
A_{2A} test set	2×2 contingency table			A_3 test set	2×2 contingency table				
			Predicted class				Predicted class		
			Active		Inactive			Active	Inactive
Actual class	Active	2	1	Actual class	Active	4	2		
	Inactive	0	7		Inactive	1	3		

Table 5

Most significant statistical parameters obtained from values included within confusion matrices, for both A_{2A} (left) and A_3 (right) models, each calculated on the basis of TR, LOO and TS, respectively

	A_{2A}			A_3		
	TR	LOO	TS	TR	LOO	TS
Sensitivity (true positive rate)	1	1	0.67	1	0.78	0.67
Specificity (true negative rate)	1	0.94	1	0.86	0.43	0.75
Concordance or accuracy	1	0.95	0.9	0.95	0.67	0.7
Positive predictivity	1	0.75	1	0.93	0.73	0.8
Positive predictivity by permutation test	0.99	—	—	0.21	—	—
Negative predictivity	1	1	0.88	1	0.5	0.6
Negative predictivity by permutation test	0.082	—	—	0.97	—	—
False positive (over-classification) rate	0	0.056	0	0.147	0.57	0.25
False negative (over-classification) rate	0	0	0.33	0	0.21	0.33
Error rate	0	0.048	0.1	0.048	0.33	0.3
NO-model error rate, NOMER%	19.05	14.28	30	66.67	66.67	60
Prior probability of active class	0.25	0.33	0.33	0.071	0.071	0.17
Prior probability of inactive class	0.059	0.056	0.14	0.14	0.14	0.25
Prior proportional probability of active class	0.19	0.14	0.3	0.67	0.67	0.6
Prior proportional probability of inactive class	0.81	0.86	0.7	0.33	0.33	0.4

represented by means of the following rules:

Rule 1:

$R\pi\text{ID-TPC} \leq 70.734$
 $\text{MIC}_0 \leq 1.56$
 \rightarrow class Active (3/1)

Rule 2:

$R\pi\text{ID-TPC} > 70.734$
 $\text{MIC}_0 \leq 1.56$
 \rightarrow class Inactive (3/0)

Rule 3:

$R\pi\text{ID-TPC} \leq 95.964$
 $\text{MIC}_0 > 1.56$
 \rightarrow class Active (12/0)

Rule 4:

$R\pi\text{ID-TPC} > 95.964$
 \rightarrow class Inactive (3/0)

The numbers in parentheses represent the number of compounds predicted to belong to the corresponding class (on the left) and the number of misclassified molecules (on the right). Descriptors involved in this model are: $R\pi\text{ID-TPC}$ and MIC_0 . $R\pi\text{ID-TPC}$ is the difference between Randic conventional bond-order (π) ID number and total path count.^{15,16} MIC_0 is Mean information content index (0-order) and it accounts for the atomic composition of the molecule.²⁰

Rule 1 ($\text{MIC}_0 \leq 1.56$ and $R\pi\text{ID-TPC} \leq 70.734$: Active (3/1)) says that the absence of any group or the presence of cyclopropyl, cyclobutyl or cyclopentyl rings are allowed, leading to an appreciable activity.

Rule 2 ($R\pi\text{ID-TPC} > 70.734$ e $\text{MIC}_0 \leq 1.56$: Inactive (3/0)) says that cyclohexyl groups or phenyl rings substituted by electron-releasing (such as alkyl) groups make a compound to be inactive.

Rule 3 ($R\pi\text{ID-TPC} \leq 95.964$ and $\text{MIC}_0 > 1.56$ Active (12/0)) says that a phenyl substitution by electron-withdrawing groups as methoxy, halogen, nitro and trifluoromethyl is allowed at meta and para positions, leading to active compounds. It should be noted that the definition of activity on this receptor is in the high nanomolar or micromolar range.

Rule 4 ($R\pi\text{ID-TPC} > 95.964$: Inactive (3/0)) says that compounds with a *ortho*-phenyl substitution by electron-withdrawing groups as alkyloxy, nitro and/or trifluoromethyl are inactive.

For this model as well, the applicability domain was calculated on the basis of descriptor range. It can be illustrated as follows: $R\pi\text{ID-TPC}$ ranges from 62.933 to 102.75, while MIC_0 ranges from 1.472 to 1.781.

Confusion matrices concerning the QSAR model for A_3 adenosine receptor are illustrated in Table 4, right column. The most significant statistical parameters for the A_3 model are reported in Table 5, right column.

5.5. Comparison of the developed QSAR models with corresponding models obtained by random selection of TR/TS pairs

Random splitting of dataset in TR and TS lead to composition summarised in Table 6.

The following equation defines the random QSAR model developed on A_1 adenosine receptor:

$$pK_i = 13.3128 - 0.0483(\pm 0.0115) * R\pi\text{ID-TPC} \\ - 262.094(\pm 86.488) * J_8$$

The applicability domain of this random model, calculated on the basis of descriptor ranges, is summarised as follows: $R\pi\text{ID-TPC}$ values: from 62.933 to 99.964 and J_8 values: from 0.006 to 0.01. Statistical parameters describing this model are reported in Table 7.

Normal distribution of variables and errors (according to the Kolmogorov–Smirnov test), as well as homoscedasticity criteria were observed (see plot in Fig. 3)

The random QSAR model developed on A_{2A} adenosine receptor is represented in the form of the rules reported below:

Rule 1:

$\text{B6HES} \leq 3.121$
 \rightarrow class Active (3/0)

Rule 2:

$\text{B6HES} > 3.121$
 \rightarrow class Inactive (18/0)

Also in this case, the applicability domain of the random model was calculated on the basis of the range of descriptor values, that is, B6HES values must range from 2.879 to 3.34. Confusion matrices concerning the random QSAR model for A_{2A} adenosine receptor are illustrated in Table 8, left column. The most significant statistical

Table 6
Summary of actual and predicted affinity values towards adenosine A₁ receptor and actual and predicted affinity class towards A_{2A} and A₃ receptors, for all the analysed compounds, together with their belonging to TR_{random} or TS_{random}, and with molecular descriptors involved in the random models

Compd ID	TR _{random} or TS _{random}	A ₁ actual pK _i	A ₁ predicted pK _i	A _{2A} actual class	A _{2A} predicted class	A ₃ actual class	A ₃ predicted class	RrID-TPC	B6HES	J ₈	MIC ₀
1	TR _{random}	8.25	8.44	Active	Active	Active	Active	62.933	2.879	0.007	1.472
2a	TS _{random}	8.12	8.39	Active	Active	Inactive	Active	63.987	3.067	0.007	1.549
2b	TS _{random}	8.65	8.49	Active	Active	Active	Active	67.39	3.107	0.006	1.532
2c	TR _{random}	8.61	8.32	Inactive	Inactive	Active	Active	70.734	3.149	0.006	1.515
2d	TR _{random}	7.91	7.9	Inactive	Inactive	Inactive	Inactive	74.013	3.193	0.007	1.498
2e	TS _{random}	8.1	7.96	Active	Active	Active	Active	78.361	3.12	0.006	1.662
2f1	TR _{random}	7.93	7.96	Active	Active	Active	Active	78.361	3.121	0.006	1.619
2f2	TR _{random}	8	7.96	Active	Active	Active	Active	78.361	3.116	0.006	1.619
2g	TR _{random}	6.96	7.35	Inactive	Inactive	Inactive	Inactive	85.568	3.16	0.007	1.521
2h1	TR _{random}	7.4	6.53	Inactive	Inactive	Active	Active	91.665	3.16	0.009	1.634
2h2	TR _{random}	7.66	7.39	Inactive	Inactive	Active	Active	84.757	3.164	0.007	1.634
2i1	TR _{random}	6.85	6.52	Inactive	Inactive	Active	Active	91.665	3.16	0.009	1.634
2i2	TS _{random}	7.16	7.39	Inactive	Inactive	Active	Active	84.757	3.162	0.007	1.634
2i3	TR _{random}	6.97	7.12	Inactive	Inactive	Active	Active	84.784	3.164	0.008	1.634
2j	TR _{random}	6.32	6.52	Inactive	Inactive	Active	Active	91.665	3.16	0.009	1.634
2k1	TS _{random}	5.82	6.25	Inactive	Inactive	Inactive	Inactive	97.355	3.16	0.009	1.576
2k2	TR _{random}	7.03	7.13	Inactive	Inactive	Active	Active	90.044	3.199	0.007	1.576
2k3	TR _{random}	7.55	7.18	Inactive	Inactive	Active	Active	83.494	3.212	0.008	1.576
2l	TR _{random}	6.15	7.12	Inactive	Inactive	Inactive	Inactive	84.784	3.203	0.008	1.507
2m1	TR _{random}	6.26	6.06	Inactive	Inactive	Active	Active	95.964	3.182	0.01	1.742
2m2	TS _{random}	6.79	6.94	Inactive	Inactive	Active	Active	88.626	3.226	0.008	1.742
2m3	TR _{random}	6.91	7	Inactive	Inactive	Active	Active	81.789	3.236	0.009	1.742
2n	TS _{random}	5.73	6.26	Inactive	Inactive	Inactive	Inactive	102.75	3.329	0.008	1.56
2o	TR _{random}	5.15	6.28	Inactive	Inactive	Inactive	Inactive	96.89	3.164	0.009	1.684
2p	TR _{random}	5.67	5.89	Inactive	Inactive	Inactive	Inactive	99.471	3.34	0.01	1.781
2q1	TR _{random}	6.68	6.13	Inactive	Inactive	Inactive	Inactive	99.964	3.334	0.009	1.674
2q2	TR _{random}	7.11	7.03	Inactive	Inactive	Active	Active	92.055	3.296	0.007	1.674
2q3	TR _{random}	7.62	7.13	Inactive	Inactive	Inactive	Active	84.68	3.286	0.008	1.674
2r1	TS _{random}	7.46	6.53	Active	Inactive	Active	Active	91.665	3.16	0.009	1.547
2r2	TS _{random}	7.5	7.39	Inactive	Inactive	Inactive	Active	84.757	3.175	0.007	1.547
2r3	TS _{random}	8.15	7.12	Inactive	Inactive	Active	Active	84.784	3.187	0.008	1.547

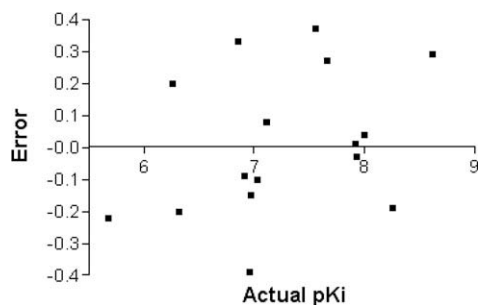


Figure 3. Plot illustrating the trend of errors versus actual pK_i values obtained by random QSAR models.

parameters for the random A_{2A} model are reported in Table 9, left column.

The random QSAR model developed on A_3 adenosine receptor can be represented by means of the following rules:

Rule 1:

$R\pi\text{ID-TPC} \leq 70.734$
 $\text{MIC}_0 \leq 1.56$
 \rightarrow class Active (2/1)

Rule 2:

$R\pi\text{ID-TPC} > 70.734$
 $\text{MIC}_0 \leq 1.52$
 \rightarrow class Inactive (3/0)

Rule 3:

$R\pi\text{ID-TPC} \leq 95.964$
 $\text{MIC}_0 > 1.52$
 \rightarrow class Active (13/1)

Rule 4:

$R\pi\text{ID-TPC} > 95.964$
 \rightarrow class Inactive (3/0)

The applicability domain for random model was calculated on the basis of descriptor range. It can be illustrated as follows: $R\pi\text{ID-TPC}$ ranges from 62.933 to 99.964, while MIC_0 ranges from 1.472 to 1.781. Confusion matrices concerning the random QSAR model for A_3 adenosine receptor are illustrated in Table 8, right column. The most significant statistical parameters for the random A_3 model are reported in Table 9, right column.

It is possible to observe, from comparison between models described in Sections 5.2–5.4 and the ones described in Section 5.5, that, in the cases investigated here, the models show satisfactory statistical parameters even when developed on a random basis.

Table 7

Model validation on adenosine A_1 receptor. Statistical parameters coming from random training set, random leave-one-out cross validation and random test set, respectively

TR_{random}		LOO_{random}		TS_{random}	
Residual sum of squares SSRES	4.23	Predictive residual sum of squares PRESS	5.32	Predictive residual sum of squares PRESS	2.59
Multiple correlation coefficient R^2	0.71	Multiple correlation coefficient Q^2	0.64	Multiple correlation coefficient R^2	0.71
Multiple correlation coefficient R^2 by permutation test	0.098	–	–	–	–
Number of predictor variables	2	Number of predictor variables	2	Number of predictor variables	2
Number of observation	21	Number of observation	21	Number of observation	10
Adjusted R^2	0.68	Adjusted Q^2	0.60	Adjusted R^2	0.62
Standard error of estimate	0.49	Standard error of prediction	0.54	Standard error of prediction	0.61
F-Value	22.55	F-Value	18.76	F-Value	8.15
Standard deviation error of estimate	0.45	Standard deviation error of prediction	0.50	Standard deviation error of prediction	0.51
		SDEP		SDEP	

Table 8

Confusion matrices concerning random QSAR models for adenosine A_{2A} (left) and A_3 (right) receptors, calculated on the basis of TR_{random} , LOO_{random} and TS_{random} , respectively

$A_{2A} TR_{\text{random}}$	2×2 contingency table			$A_3 TR_{\text{random}}$	2×2 contingency table		
	Predicted class		Predicted class				
	Active	Inactive	Active		Inactive		
Actual class	Active	3	0	Actual class	Active	14	0
	Inactive	0	18		Inactive	1	6
$A_{2A} LOO_{\text{random}}$	2×2 contingency table			$A_3 LOO_{\text{random}}$	2×2 contingency table		
	Predicted class		Predicted class				
	Active	Inactive	Active		Inactive		
Actual class	Active	2	0	Actual class	Active	11	3
	Inactive	1	18		Inactive	4	3
$A_{2A} TS_{\text{random}}$	2×2 contingency table			$A_3 TS_{\text{random}}$	2×2 contingency table		
	Predicted class		Predicted class				
	Active	Inactive	Active		Inactive		
Actual class	Active	3	1	Actual class	Active	6	0
	Inactive	0	6		Inactive	2	2

Table 9
Most significant statistical parameters obtained from values included within confusion matrices, for both A_{2A} (left) and A_3 (right) models, each calculated on the basis of TR_{random} , LOO_{random} and TS_{random} , respectively

	A_{2A}			A_3		
	TR_{random}	LOO_{random}	TS_{random}	TR_{random}	LOO_{random}	TS_{random}
Sensitivity (true positive rate)	1	1	0.75	0.93	0.78	1
Specificity (true negative rate)	1	0.95	1	1	0.43	0.5
Concordance or accuracy	1	0.95	0.9	0.95	0.67	0.8
Positive predictivity	1	0.67	1	1	0.73	0.75
Positive predictivity by permutation test	0.099	—	—	0.2	—	—
Negative predictivity	1	1	0.86	0.86	0.5	1
Negative predictivity by permutation test	0.073	—	—	0.98	—	—
False positive (over-classification) rate	0	0.053	0	0	0.57	0.5
False negative (over-classification) rate	0	0	0.25	0.067	0.21	0
Error rate	0	0.048	0.1	0.047	0.33	0.2
NO-model error rate, NOMER%	14.28	9.521	40	71.43	66.67	60
Prior probability of active class	0.33	0.5	0.25	0.067	0.071	0.17
Prior probability of inactive class	0.056	0.052	0.17	0.17	0.14	0.25
Prior proportional probability of active class	0.14	0.095	0.4	0.71	0.67	0.6
Prior proportional probability of inactive class	0.86	0.9	0.6	0.28	0.33	0.4

Thus, their performances result comparable with the models presented in Sections 5.2–5.4 and may be mechanistically interpreted in the same way, leading to same conclusions about structure–activity relationships. Nevertheless we wanted to follow two different ways, in developing QSAR models for the particular system analysed here, as in some of our previous experiences, we had found that the method described in ^{****} paragraph Sections 5.2–5.4 allowed finding better models in more complex biological systems. Of course the simplest QSAR models have to be exploited in predictive tasks.

6. Conclusions

Compounds that have been synthesised, tested and presented in this paper show high affinity for the A_1 adenosine receptor, and many of them also show a good selectivity for A_1 with respect to A_{2A} and A_3 adenosine receptors. Based on the quite rich library containing such compounds and relevant biological data, QSAR models, able to rationalise the results and to give a quantitative estimate of the observed trends were developed. The obtained models can assist in the design of new compounds selectively active on A_1 adenosine receptor, according to the general rule which can consequently be inferred: $R\pi D$ -TPC should be as low as possible, approaching the value of 70.730, within the range 70.730–95.964; MIC_0 should be in the range 1.472–1.56; $B6HES$ should be higher than 3.121, and in the range 3.121–3.34; J_8 should be as low as possible, approaching the value of 0.006, within the range 0.006–0.01.

The models suggest some structural characteristics of the binding site structure for each receptor subtype. The binding pockets of A_{2A} and A_3 receptors are expected to be slightly smaller than the one of the A_1 subtype. With regard to the ligand structural features, the group showing the highest affinity for A_1 adenosine receptor and the best selectivity A_1/A_{2A} – A_3 was found to be cyclohexyl. It should be taken as the best scaffold where different substituents at positions 3 and 4 may be introduced, in order to obtain new compounds able to modulate affinity and/or selectivity for adenosine receptors.

7. Experimental

7.1. Chemistry

Melting points were determined using a Reichert Kofler hot-stage apparatus and are uncorrected. Infrared spectra were recorded with a FT-IR spectrometer Nicolet/Avatar in Nujol mulls. Routine nuclear magnetic resonance spectra were recorded in $DMSO-d_6$ solution on a Varian Gemini 200 spectrometer operating

at 200 MHz. Mass spectra were obtained on a Hewlett–Packard 5988 A spectrometer using a direct injection probe and an electron beam energy of 70 eV. Evaporation was performed in vacuo (rotary evaporator). Analytical TLC was carried out on Merck 0.2 mm pre-coated silica gel aluminium sheets (60 F-254). Flash-column chromatography was performed using Merck Kieselgel 60 (230–400 mesh). Elemental analyses, indicated by the symbols of the elements, were performed by our Analytical Laboratory and were within $\pm 0.4\%$ of the theoretical values.

7.1.1. *N*-(9-Benzyl-2-phenyl-9H-8-azapurin-6-yl)-amides 2a–q

To a solution of 8-azaadenine **1** (100 mg, 3.3 mmol) obtained as described in the literature⁷ in 100 ml of anhydrous toluene, a solution of the suitable acyl chloride (25 mmol) in 10 ml of toluene was added drop-wise, then the mixture was refluxed for 24 h. After cooling the mixture was evaporated under reduced pressure, the residue diluted with chloroform and the solution washed with 10% NaOH, 10% HCl and water. After evaporation, the solid obtained was crystallised.

Compound 2a: yield: 18%; mp 169–170 °C (95% EtOH); IR: 3249 (NH); 1688 (C=O). ¹H NMR: 11.79 (br s, 1H exch., NH); 8.53 (m, 2H, arom); 7.60–7.36 (m, 8H, arom); 5.96 (s, 2H, CH₂–benzyl); 2.37 (s, 1H, COCH); 0.99 (m, 4H, CH₂). MS: 370 (M^+ , 10), 215 (100) m/z . Elemental analysis for C₂₁H₁₈N₆O: Calcd: C, 68.09; H, 4.90; N, 22.69. Found: C, 67.98; H, 4.86; N, 22.50.

Compound 2b: yield: 13%; mp 160–162 °C (95% EtOH); IR: 3255 (NH); 1685 (C=O). ¹H NMR: 11.31 (br s, 1H exch., NH); 8.50 (m, 2H, arom); 7.61–7.35 (m, 8H, arom); 5.95 (s, 2H, CH₂–benzyl); 3.74 (m, 1H, COCH); 2.26 (m, 4H, CH₂); 1.97 (m, 2H, CH₂). MS: 384 (M^+ , 4), 129 (100) m/z . Elemental analysis for C₂₂H₂₀N₆O: Calcd: C, 68.73; H, 5.24; N, 21.86. Found: C, 68.90; H, 5.31; N, 22.02.

Compound 2c: yield: 15%; mp 170–171 °C (95% EtOH); IR: 3284 (NH); 1693 (C=O). ¹H NMR: 11.42 (br s, 1H exch., NH); 8.51 (m, 2H, arom); 7.58–7.34 (m, 8H, arom); 5.94 (s, 2H, CH₂–benzyl); 3.28 (m, 1H, COCH); 1.97–1.62 (m, 8H, CH₂). MS: 398 (M^+ , 5), 129 (100) m/z . Elemental analysis for C₂₃H₂₂N₆O: Calcd: C, 69.33; H, 5.57; N, 21.09. Found: C, 69.48; H, 5.51; N, 21.12.

Compound 2d: yield: 13%; mp 166–167 °C (95% EtOH); IR: 3255 (NH); 1689 (C=O). ¹H NMR: 11.40 (br s, 1H exch., NH); 8.51 (m, 2H, arom); 7.57–7.34 (m, 8H, arom); 5.94 (s, 2H, CH₂–benzyl); 2.84 (m, 1H, COCH); 1.96–1.22 (m, 10H, CH₂). MS: 421 (M^+ , 5), 129 (100) m/z . Elemental analysis for C₂₄H₂₄N₆O: Calcd: C, 69.88; H, 5.86; N, 20.37. Found: C, 69.57; H, 5.51; N, 20.13.

Compound 2e: yield: 28%; mp 213–215 °C (95% EtOH); IR: 3229 (NH); 1667 (C=O). ¹H NMR: 11.92 (s, 1H exch., NH); 8.53 (m, 2H, arom); 8.27 (m, 1H, arom); 8.04 (m, 1H, arom); 7.60–7.25 (m,

9H, arom); 5.97 (s, 2H, CH₂-benzyl). MS: 412 (M⁺, 30), 189 (100) *m/z*. Elemental analysis for C₂₂H₁₆N₆O₅: Calcd: C, 64.06; H, 3.91; N, 20.38. Found: C, 63.95; H, 4.23; N, 20.22.

Compound 2f1: yield: 30%; mp 197–198 °C (95% EtOH); IR: 3326 (NH); 1689 (C=O). ¹H NMR: 11.72 (br s, 1H exch., NH); 8.54 (m, 2H, arom); 8.07 (d, *J* = 1.0 Hz, 1H, arom); 7.70 (d, *J* = 3.2 Hz, 1H, arom); 7.60–7.34 (m, 8H, arom); 6.79 (m, 1H, arom); 5.97 (s, 2H, CH₂-benzyl). MS: 396 (M⁺, 5), 233 (100) *m/z*. Elemental analysis for C₂₂H₁₆N₆O₂: Calcd: C, 66.66; H, 4.07; N, 21.20. Found: C, 66.80; H, 4.24; N, 21.28.

Compound 2f2: yield: 5%; mp 216–218 °C (95% EtOH); IR: 3126 (NH); 1685 (C=O). ¹H NMR: 11.64 (br s, 1H exch., NH); 8.67 (s, 1H, arom); 8.55 (m, 2H, arom); 7.89 (m, 1H, arom); 7.61–7.09 (m, 9H, arom); 5.98 (s, 2H, CH₂-benzyl). MS: 396 (M⁺, 2), 233 (100) *m/z*. Elemental analysis for C₂₂H₁₆N₆O₂: Calcd: C, 66.66; H, 4.07; N, 21.20. Found: C, 66.74; H, 4.21; N, 21.33.

Compound 2g: yield: 20%; mp 227–228 °C (95% EtOH); IR: 3239 (NH); 1672 (C=O). ¹H NMR: 11.95 (br s, 1H exch., NH); 8.48 (m, 2H, arom); 8.08 (d, *J* = 8.6 Hz, 2H, arom); 7.68–7.32 (m, 11H, arom); 5.91 (s, 2H, CH₂-benzyl). MS: 436 (M⁺, 5), 273 (100) *m/z*. Elemental analysis for C₂₄H₁₈N₆O: Calcd: C, 70.92; H, 4.46; N, 20.68. Found: C, 70.79; H, 4.25; N, 20.38.

Compound 2h1: yield: 80%; mp 193–194 °C (95% EtOH); IR: 3236 (NH); 1685 (C=O). ¹H NMR: 12.16 (s, 1H exch., NH); 8.21 (m, 2H, arom); 7.82–7.28 (m, 12H, arom); 5.96 (s, 2H, CH₂-benzyl). MS: 424 (M⁺, 11), 273 (100) *m/z*. Elemental analysis for C₂₄H₁₇N₆O: Calcd: C, 67.92; H, 4.04; N, 19.80. Found: C, 68.14; H, 4.20; N, 20.18.

Compound 2h2: yield: 21%; mp 210–211 °C (95% EtOH); IR: 3242 (NH); 1675 (C=O). ¹H NMR: 11.97 (s, 1H exch., NH); 8.49 (m, 2H, arom); 7.91 (m, 2H, arom); 7.56–7.34 (m, 10H, arom); 5.98 (s, 2H, CH₂-benzyl). MS: 424 (M⁺, 10), 273 (100) *m/z*. Elemental analysis for C₂₄H₁₇N₆O: Calcd: C, 67.92; H, 4.04; N, 19.80. Found: C, 68.19; H, 4.28; N, 20.01.

Compound 2h3: yield: 25%; mp 260–261 °C (95% EtOH); IR: 3252 (NH); 1674 (C=O). ¹H NMR: 11.90 (s, 1H exch., NH); 8.49 (m, 2H, arom); 8.15 (m, 2H, arom); 7.57–7.37 (m, 10H, arom); 5.99 (s, 2H, CH₂-benzyl). MS: 424 (M⁺, 9), 395 (100) *m/z*. Elemental analysis for C₂₄H₁₇N₆O: Calcd: C, 67.92; H, 4.04; N, 19.80. Found: C, 67.99; H, 4.12; N, 19.88.

Compound 2i1: yield: 15%; mp 210–211 °C (95% EtOH); IR: 3238 (NH); 1688 (C=O). ¹H NMR: 12.31 (s, 1H exch., NH); 8.09 (m, 2H, arom); 7.68–7.36 (m, 12H, arom); 5.96 (s, 2H, CH₂-benzyl). MS: 405 (31) 139 (100) *m/z*. Elemental analysis for C₂₄H₁₇ClN₆O: Calcd: C, 65.38; H, 3.89; N, 19.06. Found: C, 65.11; H, 4.12; N, 19.17.

Compound 2i2: yield: 35%; mp 219–220 °C (95% EtOH); IR: 3241 (NH); 1685 (C=O). ¹H NMR: 11.98 (br s, 1H exch., NH); 8.48 (m, 2H, arom); 8.14 (s, 1H, arom); 8.05 (d, *J* = 7.2 Hz, 1H); 7.79–7.36 (m, 10H, arom); 5.99 (s, 2H, CH₂-benzyl). MS: 440 (M⁺, 15) 178 (100) *m/z*. Elemental analysis for C₂₄H₁₇ClN₆O: Calcd: C, 65.38; H, 3.89; N, 19.06. Found: C, 65.37; H, 4.00; N, 19.21.

Compound 2i3: yield: 58%; mp 220–221 °C (95% EtOH); IR: 3259 (NH); 1674 (C=O). ¹H NMR: 11.87 (br s, 1H exch., NH); 8.35 (m, 2H, arom); 8.12 (d, *J* = 7.0 Hz, 2H, arom); 7.70–7.34 (m, 10H, arom); 5.99 (s, 2H, CH₂-benzyl). MS: 440 (M⁺, 82) 160 (100) *m/z*. Elemental analysis for C₂₄H₁₇ClN₆O: Calcd: C, 65.38; H, 3.89; N, 19.06. Found: C, 65.41; H, 3.92; N, 19.10.

Compound 2j: yield: 44%; mp 178–180 °C (95% EtOH); IR: 3201 (NH); 1665 (C=O). ¹H NMR: 12.24 (br s, 1H exch., NH); 8.11 (m, 2H, arom); 7.97 (d, *J* = 7.8 Hz, 1H); 7.56–7.32 (m, 11H, arom); 5.96 (s, 2H, CH₂-benzyl). MS: 405 (M⁺, 128, 90), 91 (100) *m/z*. Elemental analysis for C₂₄H₁₇I₂N₆O: Calcd: C, 54.15; H, 3.22; N, 15.79. Found: C, 54.31; H, 3.12; N, 15.56.

Compound 2k1: yield: 34%; mp 198–200 °C (95% EtOH); IR: 3281 (NH); 1704 (C=O). ¹H NMR: 11.70 (br s, 1H exch., NH); 8.34 (m, 2H, arom); 7.85 (d, *J* = 7.6 Hz, 1H); 7.53–7.17 (m, 11H,

arom); 5.96 (s, 2H, CH₂-benzyl); 3.86 (s, 3H, OCH₃). MS: 436 (M⁺, 8), 233 (100) *m/z*. Elemental analysis for C₂₅H₂₀N₆O₂: Calcd: C, 68.80; H, 4.62; N, 19.25. Found: C, 69.10; H, 4.87; N, 19.46.

Compound 2k2: yield: 40%; mp 179–180 °C (95% EtOH); IR: 3245 (NH); 1677 (C=O). ¹H NMR: 11.83 (br s, 1H exch., NH); 8.34 (m, 2H, arom); 7.70–7.24 (m, 12H, arom); 5.97 (s, 2H, CH₂-benzyl); 3.86 (s, 3H, OCH₃). MS: 436 (M⁺, 5), 233 (100) *m/z*. Elemental analysis for C₂₅H₂₀N₆O₂: Calcd: C, 68.80; H, 4.62; N, 19.25. Found: C, 68.99; H, 4.81; N, 19.25.

Compound 2k3: yield: 36%; mp 223–224 °C (95% EtOH); IR: 3240 (NH); 1670 (C=O). ¹H NMR: 11.81 (br s, 1H exch., NH); 8.50 (m, 2H, arom); 8.10 (d, *J* = 7.6 Hz, 2H, arom); 7.57–7.35 (m, 8H, arom); 7.11 (d, *J* = 7.6 Hz, 2H, arom); 5.97 (s, 2H, CH₂-benzyl); 3.86 (s, 3H, OCH₃). MS: 436 (M⁺, 7), 91 (100) *m/z*. Elemental analysis for C₂₅H₂₀N₆O₂: Calcd: C, 68.80; H, 4.62; N, 19.25. Found: C, 68.83; H, 4.67; N, 19.38.

Compound 2l: yield: 32%; mp > 300 °C (95% EtOH); IR: 3266 (NH); 1671 (C=O). ¹H NMR: 11.81 (br s, 1H exch., NH); 8.51 (m, 2H, arom); 8.03 (d, *J* = 3.8 Hz, 2H, arom); 7.60–7.37 (m, 10H, arom); 5.99 (s, 2H, CH₂-benzyl); 2.44 (s, 3H, CH₃). MS: 420 (M⁺, 4), 91 (100) *m/z*. Elemental analysis for C₂₅H₂₀N₆O: Calcd: C, 71.41; H, 4.79; N, 19.99. Found: C, 71.33; H, 4.86; N, 19.94.

Compound 2m1: yield: 20%; mp 178–180 °C (MeOH); IR: 3221 (NH); 1675 (C=O). ¹H NMR: 12.38 (br s, 1H exch., NH); 8.03–7.76 (m, 6H, arom); 7.52–7.35 (m, 8H, arom); 5.95 (s, 2H, CH₂-benzyl). MS: 474 (M⁺, 8), 173 (100) *m/z*. Elemental analysis for C₂₅H₁₇F₃N₆O: Calcd: C, 63.29; H, 3.61; N, 17.71. Found: C, 63.15; H, 3.47; N, 17.62.

Compound 2m2: yield: 39%; mp 210 °C dec. (95% EtOH); IR: 3235 (NH); 1679 (C=O). ¹H NMR: 12.29 (br s, 1H exch., NH); 8.49–8.35 (m, 4H, arom); 8.20 (d, *J* = 7.4, 1H, arom), 7.83 (t, *J* = 7.6 Hz, 1H, arom); 7.58–7.36 (m, 8H, arom); 5.99 (s, 2H, CH₂-benzyl). MS: 474 (M⁺, 10), 173 (100) *m/z*. Elemental analysis for C₂₅H₁₇F₃N₆O: Calcd: C, 63.29; H, 3.61; N, 17.71. Found: C, 63.45; H, 3.55; N, 17.60.

Compound 2m3: yield: 25%; mp 230–231 °C (MeOH); IR: 3247 (NH); 1672 (C=O). ¹H NMR: 12.14 (br s, 1H exch., NH); 8.48 (m, 2H, arom); 8.24 (d, *J* = 8.2 Hz, 2H, arom); 7.96 (d, *J* = 8.2 Hz, 2H, arom); 7.59–7.32 (m, 8H, arom); 5.98 (s, 2H, CH₂-benzyl). MS: 474 (M⁺, 12), 445 (100) *m/z*. Elemental analysis for C₂₅H₁₇F₃N₆O: Calcd: C, 63.29; H, 3.61; N, 17.71. Found: C, 63.57; H, 3.74; N, 17.82.

Compound 2n: yield: 11%; mp 169–170 °C (95% EtOH); IR: 3262 (NH); 1696 (C=O). ¹H NMR: 11.70 (br s, 1H exch., NH); 8.34 (m, 2H, arom); 7.93 (m, 1H, arom); 7.63–7.15 (m, 11H, arom); 5.97 (s, 2H, CH₂-benzyl); 4.13 (q, *J* = 6.8 Hz, 2H, CH₂); 1.30 (t, *J* = 6.8 Hz, 3H, CH₃). MS: 450 (M⁺, 2), 273 (100) *m/z*. Elemental analysis for C₂₆H₂₂N₆O₂: Calcd: C, 69.32; H, 4.92; N, 18.66. Found: C, 69.45; H, 4.81; N, 18.85.

Compound 2o: yield: 34%; mp 206–207 °C (95% EtOH); IR: 3283 (NH); 1701 (C=O). ¹H NMR: 11.86 (br s, 1H exch., NH); 8.29 (m, 2H, arom), 7.78 (d, *J* = 2.6 Hz, 1H, arom), 7.67–7.21 (m, 10H, arom), 5.98 (s, 2H, CH₂-benzyl), 3.80 (s, 3H, CH₃). MS: 471 (M⁺, 2), 436 (100) *m/z*. Elemental analysis for C₂₅H₁₉ClN₆O₂: Calcd: C, 63.76; H, 4.07; N, 17.85. Found: C, 63.54; H, 4.02; N, 17.98.

Compound 2p: yield: 40%; mp 175–176 °C (95% EtOH); IR: 3227 (NH); 1682 (C=O). ¹H NMR: 12.59 (s, 1H exch., NH); 8.42 (s, 1H, arom), 8.07–7.86 (m, 4H, arom), 7.56–7.36 (m, 8H, arom), 5.96 (s, 2H, CH₂-benzyl). MS: 485 (M⁺, 20), 215 (100) *m/z*. Elemental analysis for C₂₄H₁₆ClN₇O₃: Calcd: C, 59.33; H, 3.32; N, 20.18. Found: C, 59.21; H, 3.55; N, 20.05.

Compound 2q1: yield: 30%; mp 195–196 °C (95% EtOH); IR: 3234 (NH); 1682 (C=O). ¹H NMR: 12.51 (br s, 1H exch., NH); 8.30 (m, 2H, arom); 7.98–7.29 (m, 12H, arom); 5.95 (s, 2H, CH₂-

benzyl). MS: 451 (M^+ , 2), 149 (100) m/z . Elemental analysis for $C_{24}H_{17}N_7O_3$: Calcd: C, 63.85; H, 3.80; N, 21.72. Found: C, 63.91; H, 3.60; N, 21.48.

Compound 2q2: yield: 22%; mp 185–186 °C (isopropanol); IR: 3225 (NH); 1669 (C=O). 1H NMR: 12.27 (br s, 1H exch., NH); 8.91 (s, 1H, arom); 8.51 (m, 4H, arom); 7.89 (t, $J = 8$ Hz, 1H, arom); 7.59–7.33 (m, 8H, arom); 5.99 (s, 2H, CH_2 -benzyl). MS: 451 (M^+ , 4), 150 (100) m/z . Elemental analysis for $C_{24}H_{17}N_7O_3$: Calcd: C, 63.85; H, 3.80; N, 21.72. Found: C, 63.58; H, 3.99; N, 21.93.

Compound 2q3: yield: 30%; mp 245–246 °C (isopropanol); IR: 3311 (NH); 1705 (C=O). 1H NMR: 12.25 (br s, 1H exch., NH); 8.43–8.27 (m, 6H, arom); 7.57–7.36 (m, 8H, arom); 5.99 (s, 2H, CH_2 -benzyl). MS: 451 (M^+ , 5), 149 (100) m/z . Elemental analysis for $C_{24}H_{17}N_7O_3$: Calcd: C, 63.85; H, 3.80; N, 21.72. Found: C, 63.60; H, 3.52; N, 21.99.

7.1.2. *N*-(9-Benzyl-2-phenyl-9H-8-azapurin-6-yl)-amides 2r1–2r3

Compounds **2q1–3** (0.2 mmol) were hydrogenated over 10% Pd/C (20 mg) in EtOH (250 ml) at room pressure and temperature. After filtration, the solvent was evaporated to give the desired compound that was crystallised from isopropanol.

Compound 2r1: yield: 85%; mp 166–167 °C; IR: 3471, 3363, 3262 (NH); 1667 (C=O). 1H NMR: 11.3 (br s, 1H exch., NH); 8.50 (m, 2H, arom); 7.95–7.20 (m, 12H, arom); 6.16 (br s, 2H exch., NH_2); 5.96 (s, 2H, CH_2 -benzyl). MS: 421 (M^+ , 5), 273 (100) m/z . Elemental analysis for $C_{24}H_{19}N_7O_3$: Calcd: C, 68.40; H, 4.54; N, 23.26. Found: C, 68.45; H, 4.70; N, 23.23.

Compound 2r2: yield: 95%; mp 221–222 °C; IR: 3395, 3313, 3160 (NH); 1639 (C=O). 1H NMR: 11.59 (br s, 1H exch., NH); 8.50 (m, 2H, arom); 7.59–7.16 (m, 11H, arom); 6.84 (m, 1H, arom); 5.97 (s, 2H, CH_2 -benzyl); 5.40 (br s, 2H exch., NH_2). MS: 421 (M^+ , 45), 332 (100) m/z . Elemental analysis for $C_{24}H_{19}N_7O_3$: Calcd: C, 68.40; H, 4.54; N, 23.26. Found: C, 68.61; H, 4.35; N, 23.55.

Compound 2r3: yield: 85%; mp 208–210 °C; IR: 3290 (NH); 1678 (C=O). 1H NMR: 11.2 (br s, 1H exch., NH); 8.51 (m, 2H, arom); 7.84 (d, $J = 8.6$ Hz, 2H, arom); 7.59–7.35 (m, 8H, arom); 6.63 (d, $J = 8.6$ Hz, 2H, arom); 6.07 (s, 2H exch., NH_2); 5.95 (s, 2H, CH_2 -benzyl). MS: 421 (M^+ , 14), 273 (100) m/z . Elemental analysis for $C_{24}H_{19}N_7O_3$: Calcd: C, 68.40; H, 4.54; N, 23.26. Found: C, 68.66; H, 4.45; N, 23.52.

7.2. Biological assays

7.2.1. Materials

$[^3H]$ DPCPX (120 Ci/mmol) was purchased from Amersham Pharmacia, $[^3H]$ NECA (20.6 Ci/mmol), was from PerkinElmer Live Science. $[^3H]$ ZM241385 (27.4 Ci/mmol) was from Tocris Cookson. DPCPX, NECA and CPA were from Sigma–Aldrich. All other chemicals used, at analytical grade, were from standard commercial sources.

7.2.2. Radioligand binding assays

Membranes of rat cerebral cortex which express A_1 adenosine receptors were prepared by using the method described by Lohse et al.²¹ with slight modifications. Male Wistar rat brain cortex was homogenised in 10 volumes of ice-cold 0.32 M sucrose, 20 mM Tris–HCl buffer pH 7.4 with 30 strokes in Dounce homogeniser. The homogenate was centrifuged at 1000g for 10 min to remove the nuclear fraction, and the resulting supernatant was centrifuged at 30,000g for 30 min. The pellet was re-suspended using 10 strokes in Dounce homogeniser in 10 volumes of ice-cold 5 mM Tris–HCl buffer pH 7.4 for 30 min. After 60 strokes in Dounce homogeniser, the resulting synaptosomal membranes were preincubated for 30 min at 37 °C with 2 U/ml of adenosine deaminase to

remove endogenous adenosine. The membrane suspension was then centrifuged at 48,000g for 30 min, and the resulting pellet was re-suspended in 10 volumes of 50 mM Tris–HCl buffer pH 7.4, and stored at –80 °C until binding assays were made.

For displacement experiments involving A_1 adenosine receptors, rat cortex membranes (40 mg of protein) were incubated at 25 °C for 60 min with $[^3H]$ DPCPX 0.5 nM ($K_d = 0.4$ nM), and increasing concentrations of the compounds, in a final volume of 0.4 ml of Tris–HCl buffer. Non-specific binding was measured in the presence of 100 μ M CPA. Binding reactions were terminated by dilution with ice-cold 50 mM Tris–HCl buffer pH 7.4. Samples were then filtered through Whatman GF/C glass-fibre filters using a Brandel cell harvester. Filters were washed three times with 4 ml of the same buffer. Bound radioactivity was measured in a liquid scintillation counter (1600 TR Packard) after the addition of 4 ml of scintillation liquid (Emulsifier-Safe, Packard).

Slightly different conditions were set in the case of binding displacement experiments regarding A_{2A} and A_3 adenosine receptors. Membranes of CHO cells expressing recombinant human A_{2A} or A_3 receptors were prepared as previously described.⁵ Membranes (40 mg of protein) were incubated with $[^3H]$ ZM241385 6 nM ($K_d = 4$ nM) in the experiments involving the A_{2A} subtype, and $[^3H]$ NECA 15 nM ($K_d = 150$ nM) in the ones involving the A_3 subtype, and the compounds to be assayed, at fixed concentration (10 μ M) or at increasing concentrations of the compounds in duplicate, in a final volume of 0.4 ml of Tris–HCl buffer for 120 min at 25 °C. Non-specific binding was measured in the presence of 100 μ M NECA in the case of A_{2A} , and 100 μ M R-PIA in the case of A_3 binding assay.

Samples were handled as mentioned before.

Binding parameters were calculated by GRAPHPAD PRISM software (GRAPHPAD, San Diego, CA, USA).

Acknowledgement

This research was supported by the Italian Ministero dell'Istruzione, dell'Università e della Ricerca (MIUR).

References and notes

- Fredholm, B. B.; Ijzerman, A. P.; Jacobson, K. A.; Klotz, K. N.; Linden, J. *Pharmacol. Rev.* **2001**, *53*, 527.
- Jacobson, K. A.; Gao, Z.-G. *Nat. Rev. Drug Discovery* **2006**, *5*, 247.
- Biagi, G.; Giorgi, I.; Livi, O.; Scartoni, V. *Farmaco* **1996**, *51*, 395.
- Biagi, G.; Giorgi, I.; Livi, O.; Nardi, A.; Pacchini, F.; Scartoni, V.; Lucacchini, A. *Eur. J. Med. Chem.* **2003**, *38*, 983.
- Biagi, G.; Giorgi, I.; Leonardi, M.; Livi, O.; Nardi, A.; Pacchini, F.; Scartoni, V.; Costa, B.; Lucacchini, A. *Eur. J. Med. Chem.* **2003**, *38*, 801.
- Giorgi, I.; Bianucci, A. M.; Biagi, G.; Livi, O.; Scartoni, V.; Leonardi, M.; Pietra, D.; Coi, A.; Massarelli, I.; Ahmad Nofal, F.; Fiamingo, F. L.; Anastasi, P.; Giannini, G. *Eur. J. Med. Chem.* **2007**, *42*, 1.
- Biagi, G.; Bianucci, A. M.; Coi, A.; Giorgi, I.; Livi, O.; Pacchini, F.; Scartoni, V.; Costa, B.; Fabbri, L.; Micco, L.; Santini, E.; Leonardi, M.; Ahmad Nofal, F.; Salerni, O. L.-R. *Bioorg. Med. Chem.* **2005**, *13*, 4679.
- Barilli, P. L.; Biagi, G.; Livi, O.; Scartoni, V. *J. Heterocycl. Chem.* **1985**, *22*, 1607.
- Biagi, G.; Giorgi, I.; Livi, O.; Scartoni, V.; Lucacchini, A.; Martini, C.; Tacchi, P. V. *Farmaco* **1994**, *49*, 187.
- Smirnov, N. V. *Bull. Moscow Univ.* **1939**, *2*, 3.
- Demsar, J.; Zupan, B. Orange: from experimental machine learning to interactive data mining. Website <http://www.aillab.si/orange/>.
- Witten, I. H.; Frank, E. In *Data Mining. Practical Machine Learning Tools and Techniques*; Gray, J., Ed., 2nd Ed.; Morgan Kaufmann, 2005.
- Cooper, J. A.; Saracci, R.; Cole, P. *Brit. J. Cancer* **1979**, *39*, 87.
- Jaworska, J.; Nikolova-Jeliazkova, N.; Aldenberg, T. *ATLA* **2005**, *33*, 445.
- Rücker, G.; Rücker, C. *J. Chem. Inf. Comput. Sci.* **2000**, *40*, 99.
- Randic, M.; Jurs, P. C. *Quant. Struct.-Act. Relat.* **1989**, *8*, 39.
- Gilvez, J.; Garcia, R.; Salabert, M. T.; Soler, R. *J. Chem. Inf. Comput. Sci.* **1994**, *34*, 520.
- Burden, F. R. *J. Chem. Inf. Comput. Sci.* **1989**, *29*, 225.
- Burden, F. R. *Quant. Struct.-Act. Relat.* **1997**, *16*, 309.
- Basak, S. C. In *Practical Applications of Quantitative Structure–Activity Relationships (QSAR) in Environmental Chemistry and Toxicology*; Karcher, W., Devillers, J., Eds.; Kluwer Academic, 1990.
- Lohse, M. J.; Lenschow, V.; Schwabe, U. *Naunyn-Schmiedeberg's Arch. Pharmacol.* **1984**, *326*, 69.